Protein Science (1999), *8*:2234–2244. Cambridge University Press. Printed in the USA.

The turn sequence directs β-strand alignment in designed β-hairpins

EVA DE ALBA,[1] MANUEL RICO, AND M. ANGELES JIMÉNEZ

Instituto de Estructura de la Materia, Consejo Superior de Investigaciones Científicas, Serrano 119, 28006 Madrid, Spain

(RECEIVED February 19, 1999; ACCEPTED July 9, 1999)

Abstract

A previous NMR investigation of model decapeptides with identical β-strand sequences and different turn sequences demonstrated that, in these peptide systems, the turn residues played a more predominant role in defining the type of β-hairpin adopted than cross-strand side-chain interactions. This result needed to be tested in longer β-hairpin forming peptides, containing more potentially stabilizing cross-strand hydrogen bonds and side-chain interactions that might counterbalance the influence of the turn sequence. In that direction, we report here on the design and ^{1}H NMR conformational study of three β-hairpin forming pentadecapeptides. The design consists of adding two and three residues at the N- and C-termini, respectively, of the previously studied decapeptides. One of the designed pentadecapeptides includes a potentially stabilizing R-E salt bridge to investigate the influence of this interaction on β-hairpin stability. We suggest that this peptide self-associates by forming intermolecular salt bridges. The other two pentadecapeptides behave as monomers. A conformational analysis of their ^{1}H NMR spectra reveals that they adopt different types of β-hairpin structure despite having identical strand sequences. Hence, the β-turn sequence drives β-hairpin formation in the investigated pentadecapeptides that adopt β-hairpins that are longer than the average protein β-hairpins. These results reinforce our previous suggestion concerning the key role played by the turn sequence in directing the kind of β-hairpin formed by designed peptides.

Keywords: β-hairpin conformation; β-turn; NMR; peptide design; protein folding; salt bridges; side-chain interactions

The conformational behavior of protein fragments and designed peptides has long been investigated to get insights into the formation of secondary structure in the early stages of protein folding (Kim & Baldwin, 1990; Dyson & Wright, 1991, 1993). These kinds of studies are also central for the rational design of artificially built protein scaffolds able to incorporate different biochemical functions (Smith & Regan, 1997). A large amount of information about the factors involved in the formation and stability of α-helices is now available (Scholtz & Baldwin, 1992; Lyu et al., 1993; Zhou et al., 1993; Muñoz & Serrano, 1994a; Baldwin, 1995; Aurora & Rose, 1998). Experimental data on peptides adopting β-sheet motifs are, however, scarce. Alcohol-water mixtures were shown to promote the formation of native β-hairpin structures in protein fragments that do not adopt ordered structures in pure water (Cox et al., 1993; Blanco et al., 1994a; Searle et al., 1996). The formation of β-hairpins has also been reported for designed peptides containing non-natural amino acids (Gellman, 1998) as well as model systems using nonpeptide templates to bring the two strands together (LaBrenz & Kelly, 1995; Nesloney & Kelly, 1996; Gellman, 1998). However, only recently a protein fragment (Blanco et al., 1994b) and some designed peptides (Blanco et al., 1993; de Alba et al., 1995, 1996, 1997a, 1997b; Ramírez-Alvarado et al., 1996, 1997; Maynard & Searle, 1997; Smith & Regan, 1997; Blanco et al., 1998; Gellman, 1998; Maynard et al., 1998) were shown to fold into β-hairpins in aqueous solution.

β-Hairpin motifs differ in the length of the loop region connecting the two antiparallel β-strands and are classified into different types according to the number of residues taking part in the turn and the number of interstrand hydrogen bonds between the residues flanking the turn (Sibanda & Thornton, 1985, 1991; Sibanda et al., 1989). The NMR investigation of a series of decapeptides having the same amino acid sequences in the strands but different residues in the turn allowed us to demonstrate that, in these peptides, the turn sequence determines the type of β-hairpin to be formed (de Alba et al., 1997a, 1997b). We concluded that, in the

Reprint requests to: M. Angeles Jiménez, Instituto de Estructura de la Materia, Consejo Superior de Investigaciones Científicas, Serrano 119, 28006 Madrid, Spain; e-mail: angeles@malika.iem.csic.es.

[1]Current address: Laboratory of Biophysical Chemistry, National Heart, Lung and Blood Institute, National Institutes of Health, Bethesda, Maryland 20892-0380.

Abbreviations: 1D, one-dimensional; 2D, two-dimensional; $\Delta\delta_{C\alpha H}$, CαH conformational shift; COSY, homonuclear correlated spectroscopy; M_{av}, averaged molecular weight; M_{th}, theoretical molecular weight; NMR, nuclear magnetic resonance; NOE, nuclear Overhauser effect; NOESY, nuclear Overhauser enhancement spectroscopy; ppm, parts per million; RMSD, root-mean-square deviation; ROESY, rotating frame NOE spectroscopy; TOCSY, total correlation spectroscopy; TSP, sodium [3-trimethylsilyl 2,2,3,3-^{2}H] propionate.

decapeptide system, differences in turn conformation lead to changes in the β-hairpin structure even when this causes a different β-strand residue pairing and backbone-hydrogen bond register. The β-strands in our decapeptide models are only three residues long, thus the number of interstrand hydrogen bonds and favorable cross-strand side-chain interactions that may contribute to the stability and discrimination of the different kinds of β-hairpins is small. Would the turn region still dictate the type of β-hairpin adopted in longer β-strands, where the number of potentially favorable cross-strand side-chain interactions is larger?

To address this question, we proceeded to design two β-hairpin forming pentadecapeptides using two of our previous β-hairpin forming decapeptides as templates (peptides 1 and 2 in Fig. 1; de Alba et al., 1996, 1997a). These decapeptides were selected because they fold into different types of β-hairpin structures in spite of only differing in the turn sequence. Segments 3–12 of the new peptides 3 and 4 (Fig. 1) coincide with the sequences of peptides 1 and 2, respectively. Therefore, if peptide 3 were to fold into a 3:5 β-hairpin as does peptide 1 and if peptide 4 were to adopt a mixture of two 2:2 β-hairpins as does peptide 2 (Fig. 2; de Alba et al., 1997a, 1997b), this would suggest that the turn sequence also directs the type of β-hairpin adopted by these longer peptides. Furthermore, to investigate if salt bridges can stabilize β-hairpins as they do in α-helices (Marqusee & Baldwin, 1987; Merutka & Stellwagen, 1991; Scholtz & Baldwin, 1992; Scholtz et al., 1993; Baldwin, 1995), we designed a pentadecapeptide including a cross-strand side-chain salt bridge (peptide 5 in Fig. 1) using peptide 1 as a template (Fig. 1; de Alba et al., 1996, 1997a). The conformational behavior of the three designed pentadecapeptides was analyzed by ^{1}H NMR.

Results

Peptide design

Pentadecapeptides 3 and 5 were designed by adding two and three residues at the N- and C-termini, respectively, of the β-hairpin forming decapeptide 1 (de Alba et al., 1996; Fig. 1), which was taken as a template. In the 3:5 β-hairpin expected to be adopted by pentadecapeptides 3 and 5, one of the new residues will face Ile, an unpaired amino acid in the 3:5 β-hairpin formed by peptide 1 (Fig. 2A). The remaining four residues will lead to two additional interstrand pair interactions. The selection of the five new residues was based on amino acid β-sheet propensities and solubility criteria. Not all the new β-strand positions can be filled with the best β-sheet formers since the hydrophobicity of most could decrease peptide solubility or promote its aggregation tendency. The sequence VTE that is located at the C-terminus of pentadecapeptides 3 and 5 contains two residues (V and T) with high intrinsic β-sheet propensities (Chou & Fasman, 1974; Kim & Berg, 1993; Minor & Kim, 1994; Muñoz & Serrano, 1994b; Smith et al., 1994; Swindells et al., 1995) and a charged residue (E) included to improve peptide solubility. In this way, peptides 3 and 5 (Fig. 1) contain an additional TXT motif, which is supposed to be β-sheet stabilizing (Cox et al., 1993; Blanco et al., 1994a; Searle et al., 1995; de Alba et al., 1996). The S residue was introduced at the N-strand because it is the most hydrophilic amino acid with some β-sheet propensity. Charged interactions stabilize peptide structure. In β-hairpins, an interaction between the positively charged N-terminal amino group and the negatively charged C-terminal carboxylate group was shown to contribute to β-hairpin stability (de Alba et al., 1995). Cross-strand charged–charged pairs (DK, DR, EK, and ER) are statistically favored in antiparallel β-sheets (Lifson & Sander, 1980; Wouters & Curmi, 1995; Gunasekaran et al., 1997; Hutchinson et al., 1998). Likewise in α-helices, salt bridges of the type R-E (i, $i + 4$) and K-E (i, $i + 4$) are known to be stabilizing (Marqusee & Baldwin, 1987; Merutka & Stellwagen, 1991; Scholtz & Baldwin, 1992; Scholtz et al., 1993; Baldwin, 1995). Therefore, it was reasonable to expect β-hairpin stabilization by a salt bridge between facing residues in the β-strands. Furthermore, peptides cycled through disulfide bridges located at the strand termini have been reported to form β-hairpin structures (Rietman et al., 1996; McDonnell et al., 1997), while the structure disappears in the absence of the disulfide bond (Rietman et al., 1996). Thus, a stabilizing interaction at the strand termini could favor β-hairpin formation. For all these reasons, in the case of peptide 5, an R residue was located at position 1 that would allow the formation of an R-E salt bridge in the expected 3:5 β-hairpin (Fig. 2A), leaving S at position 2. In contrast, peptide 3 was designed to be highly soluble by locating the S residue at position 1 and introducing an E residue at position 2. In this way, the peptide has a net negative charge of −3 at high pH values. Furthermore, in the expected 3:5 β-hairpin (Fig. 2A), the two E side chains will point toward different sides of the β-sheet plane, so that both β-hairpin faces will present a similar polarity.

For comparison with previous results, we used the same turn sequences in the pentadecapeptides that have produced the most strikingly different β-hairpin structures in the decapeptides (de Alba et al., 1997a). We performed the turn change on penta-

Peptide 1			I	Y	S	**N**	**P**	**D**	**G**	**T**	W	T	
Peptide 2			I	Y	S	**Y**	**N**	**G**	**K**	T	W	T	
Peptide 3	S	E	I	Y	S	**N**	**P**	**D**	**G**	**T**	W	T	V T E
Peptide 4	S	E	I	Y	S	**Y**	**N**	**G**	**K**	T	W	T	V T E
Peptide 5	R	S	I	Y	S	**N**	**P**	**D**	**G**	**T**	W	T	V T E

Fig. 1. Peptide sequences. Turn residues are in bold. The residues that lengthen peptides 3–5 relative to peptides 1–2 are underlined.

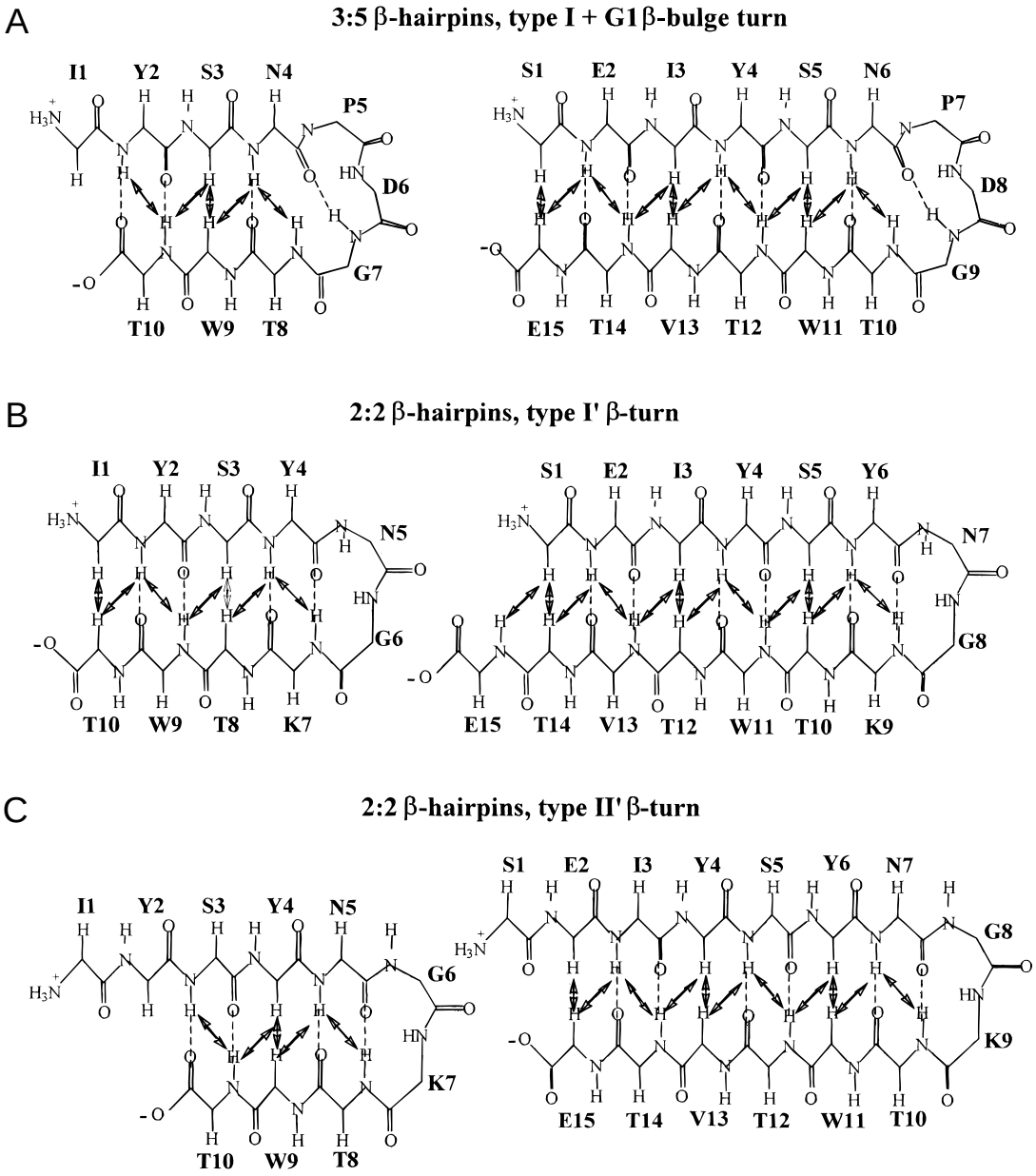

Fig. 2. Schematic representation of the peptide backbone conformations of (**A**) the 3:5 β-hairpin with a type I + G1 β-bulge turn formed by peptide 1 (left) and expected for peptides 3 and 5 (right); sequence of peptide 3 is shown; residues 1 and 2 in peptide 5 are R and S, respectively; (**B**) the 2:2 β-hairpin with a type I′ turn adopted by peptide 2 (left) and expected for peptide 4 (right); and (**C**) the 2:2 β-hairpin with a type II′ turn peptide 2 (left) and expected for peptide 4 (right). The dotted lines indicate the β-sheet hydrogen bonds and the black arrows the expected long-range NOEs involving backbone protons.

decapeptide 3 (to give peptide 4), but not on 5, because peptide 5 aggregates (see below). As in the case of peptide 2 relative to peptide 1, the sequence of peptide 4 corresponds to the substitution of the turn residues NPDG of peptide 3 by YNGK (Fig. 1). If turn sequence were crucial in defining the type of β-hairpin to be formed, peptide 4 should present the same conformational behavior as decapeptide 2. In this case, peptide 4 is expected to adopt a mixture of two 2:2 β-hairpins, one with a type I′ turn (residues YNGK) and the other with a type II′ turn (residues NGKT), as found in peptide 2 (de Alba et al., 1997a).

Aggregation state

The 1D ^{1}H NMR spectra of peptide 3 at 2 mM concentration and of peptide 4 at its maximal solubility in aqueous solution (slightly less than 1 mM) are identical in line widths and chemical shifts to those acquired at 0.1 mM concentration of peptides 3 and 4, respectively. This indicates the absence of aggregation in both peptides. To further check their monomeric state, sedimentation equilibrium experiments were performed with the concentrated samples. The similarity between the averaged molecular weight

(M_{av}) obtained by this method and the molecular weight calculated on the basis of the amino acid composition (M_{th}) indicates that both peptides are monomeric ($M_{th}/M_{av} = 1.1$ for peptide 3 and 1.0 for peptide 4).

In contrast to peptides 3 and 4, the 1D ^{1}H NMR spectra of peptide 5 in aqueous solution at 2 mM, pH 4.3, and 5 °C (data not shown) contained broad signals as well as the resonances of two conformational species. In the 1D spectrum recorded at the same pH and temperature but at a very low peptide concentration (0.1 mM), the very broad signals corresponding to the minor species disappear and those of the major species sharpen. To find experimental conditions where only one of the species was present, we tested a wide range of pH values, temperatures, and sample concentrations. At pH 4.3 and 5 °C, the very broad signals belonging to the minor species are present even at 0.5 mM, the lowest sample concentration for recording 2D spectra with an acceptable signal to noise ratio. At 2 mM peptide concentration, the major species signals sharpened and the minor ones disappear only at very acid or basic pH values (pH 2.2 or 9.4) or at high temperature (35 °C). All these results indicate the presence of aggregated states, and in particular that the concentrated sample of peptide 5 contains two different states of association in a slow equilibrium within the NMR time scale. The minor species likely corresponds to a higher degree of self-association since its population decreases when the peptide concentration is reduced. In turn, it is probable that the major species corresponds to the monomeric state. To check this hypothesis, sedimentation equilibrium experiments were performed at experimental conditions where only the major species is present (2 mM peptide concentration, 8 °C, and pH 2.2). Under these conditions, the average molecular weight (M_{av}) obtained by sedimentation equilibrium and the molecular weight calculated on the basis of the amino acid composition (M_{th}) are identical within experimental error ($M_{th}/M_{av} = 1.1$; see Fig. 1 in Supplementary material in Electronic Appendix). This indicates that the major species of peptide 5 is the monomeric state. In contrast, the averaged molecular weight (M_{av} = 2,110 g/mol) obtained by sedimentation equilibrium at 2 mM peptide concentration, pH 4.3 and 8 °C, where the population of the minor species is relatively high, is ~400 g/mol higher than the molecular weight calculated on the basis of the amino acid composition (M_{th} = 1,727 g/mol). Fitting the experimental sedimentation equilibrium data at pH 4.3 to a function corresponding to a monomeric behavior gives rise to nonrandom residuals (Fig. 2 in Supplementary material in Electronic Appendix), which are characteristic of self-association processes (McRorie & Voelker, 1993). All these results agree with the minor species being a self-associated state.

^{1}H NMR analysis

The ^{1}H NMR assignment of peptides 3 and 4 in aqueous solution and of peptide 3 in the mixed solvent TFE/H_2O (30:70) was straightforward by the standard sequential assignment procedure (Wüthrich et al., 1984; Wüthrich, 1986). ^{1}H δ-values of the two peptides are available in Supplementary material in Electronic Appendix (Tables 1, 2).

The same procedure was used to assign the ^{1}H NMR signals of monomeric peptide 5 (2 mM, pH 2.2, and 5 °C) and the resonances corresponding to the major species present at pH 4.3, 2 mM, and 8 °C. Once assigned the major species, the exchange cross peaks observed in NOESY and ROESY spectra allowed the assignment of the minor species. Cross peaks arising from chemical exchange are unambiguously identified by their negative sign in ROESY experiments, whereas true NOE cross peaks are positive. NOESY and ROESY spectral regions showing exchange cross peaks corresponding to NH protons and to methyl groups of I3 and V13, respectively, are given in Figure 3. ^{1}H δ-values at pH 2.2 and 4.3 are available in Supplementary material in Electronic Appendix (Table 3).

The most conclusive NMR evidence for the formation of β-hairpin structures comes from NOE data. Since different NOEs involving backbone protons $d_{\alpha\alpha(i,j)}$, $d_{\alpha N(i,j+1)}$, and $d_{NN(i+1,j-1)}$ are expected for different types of β-hairpin structures (Fig. 2), the set of NOEs observed allows the unambiguous identification of the strand register and the type of β-hairpin formed by a given peptide. The NOE data described here come from joint analysis of NOESY and

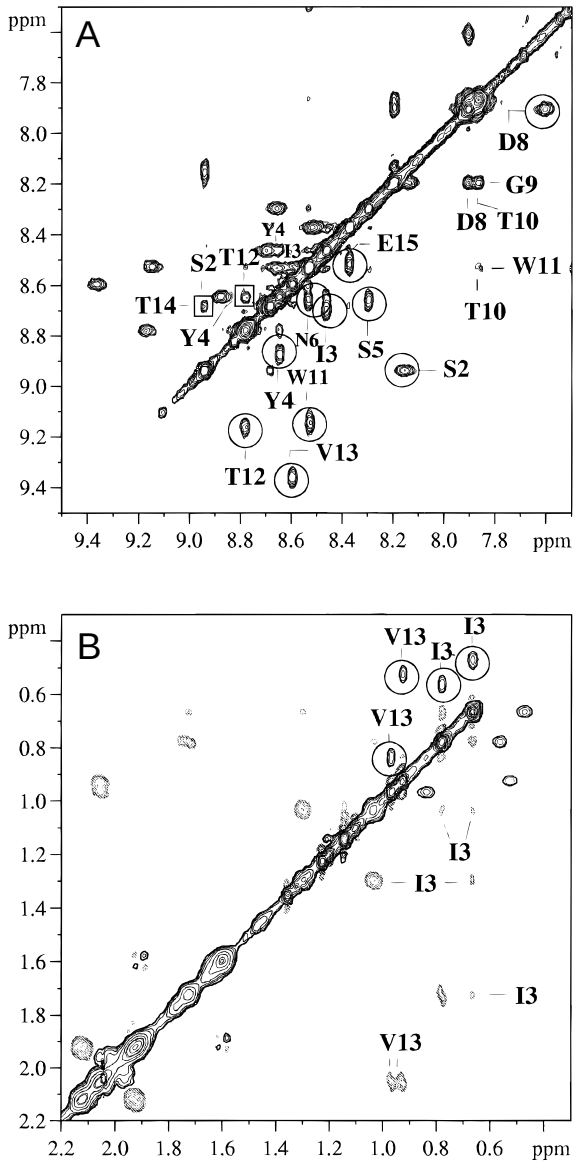

Fig. 3. (**A**) NOESY and (**B**) ROESY spectral regions of peptide 5 (2 mM, H_2O/D_2O 9:1 pH 4.3, 8 °C, 200 ms mixing time). Nonsequential cross peaks are boxed and exchange cross peaks circled. Positive contour levels at ROESY spectrum **B** are indicated by dotted lines.

ROESY spectra recorded under the same experimental conditions. ROESY experiments allow to check whether a particular cross peak corresponds to a true NOE connectivity or to spin diffusion processes. Additional information on the formation of β-hairpin structures is provided by CαH conformational shifts ($\Delta\delta_{C\alpha H} = \delta_{observed} - \delta_{random\ coil}$) (Bundi & Wüthrich, 1979) and $^3J_{\alpha N}$ coupling constants. The CαH conformational shifts ($\Delta\delta_{C\alpha H}$) are expected to be negative in the turn region and positive in the β-strand regions (Wishart & Sykes, 1994; Case et al., 1994). Nevertheless, $\Delta\delta_{C\alpha H}$ must be interpreted with caution because aromatic residues can affect chemical shifts due to ring current effects. In addition, N- and C-terminal residues are not considered for this analysis due to charged-end effects. Regarding the $^3J_{\alpha N}$ coupling constants, values greater than 8 Hz are characteristic of extended structures such as the β-strands.

Peptide 3 adopts the expected 3:5 β-hairpin conformation

The long-range NOEs involving backbone protons, NH E2-NH T14, NH N6-NH T10, CαH S5-CαH W11, and CαH S5-NH T12 (Fig. 4A,B), observed for peptide 3 in aqueous solution indicate the formation of the expected 3:5 β-hairpin (Fig. 2A). Other long-range backbone NOEs characteristic of the 3:5 β-hairpin could not be observed in aqueous solution because of signal overlap that persisted at all the pH values and temperatures tested. Only the very external nonobserved NH E2-CαH E15 NOE was in a clean spectral region. Long-range NOEs involving side-chain protons of facing residues in the 3:5 β-hairpin were also found for peptide 3 (Table 4 in Supplementary material in Electronic Appendix). In the case of decapeptide 1, in addition to the 3:5 structure, a very low, just above the signal to noise ratio, population of a 4:4 β-hairpin conformation was detected (de Alba et al., 1996). These two β-hairpin structures have completely different β-strand registers. No NOE indicative of such 4:4 β-hairpin was detected for pentadecapeptide 3, even though one of the most characteristic NOEs, CαH Y4-CαH W11, would not have overlapped with any other signal had it been present. The CαH conformational shifts observed for peptide 3 are negative in the turn region and positive in the strands, except for S5, as expected for β-hairpin structures (Fig. 5). The negative $\Delta\delta_{C\alpha H}$ value found for S5 can be explained

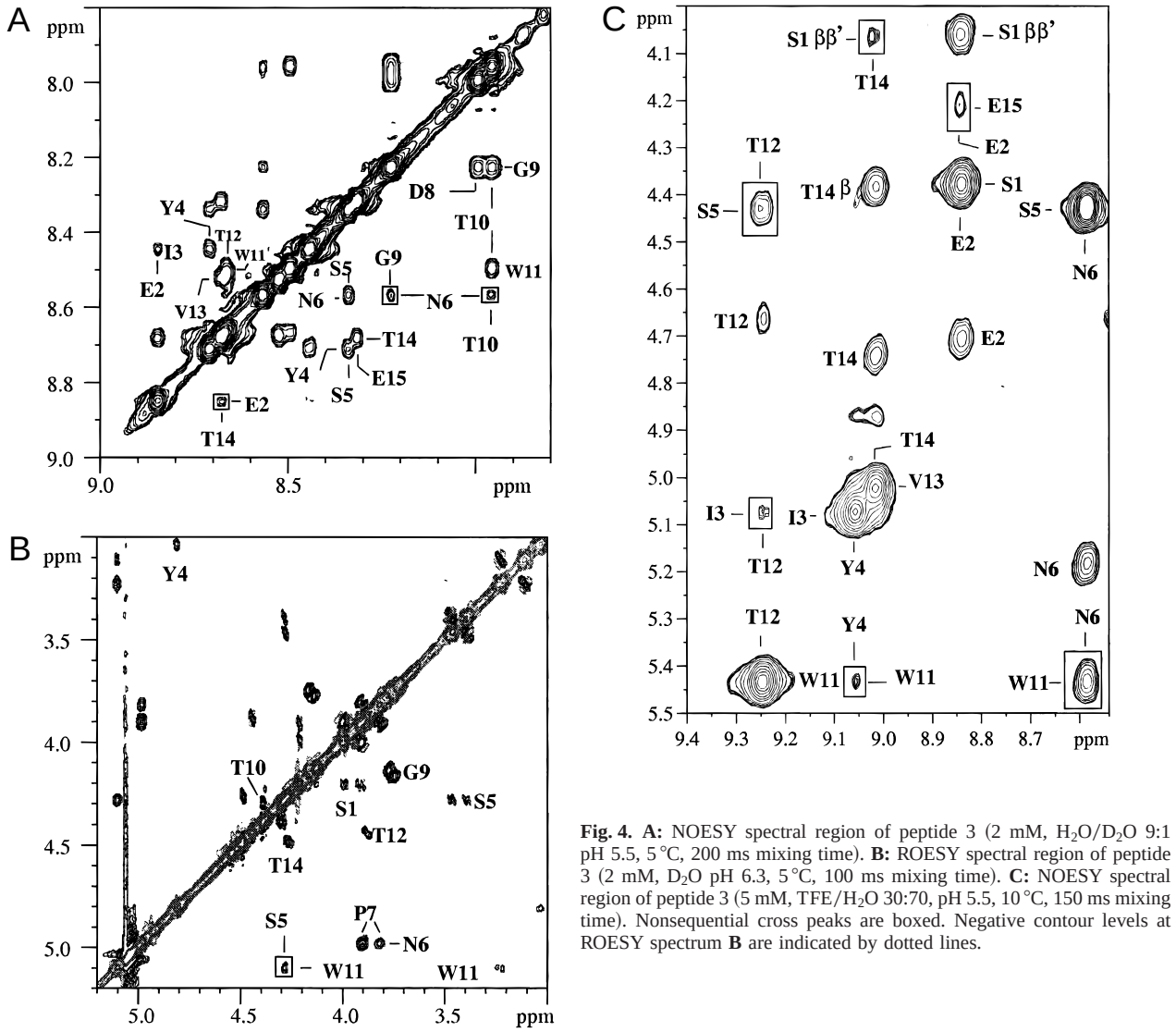

Fig. 4. A: NOESY spectral region of peptide 3 (2 mM, H_2O/D_2O 9:1 pH 5.5, 5 °C, 200 ms mixing time). **B:** ROESY spectral region of peptide 3 (2 mM, D_2O pH 6.3, 5 °C, 100 ms mixing time). **C:** NOESY spectral region of peptide 3 (5 mM, TFE/H_2O 30:70, pH 5.5, 10 °C, 150 ms mixing time). Nonsequential cross peaks are boxed. Negative contour levels at ROESY spectrum **B** are indicated by dotted lines.

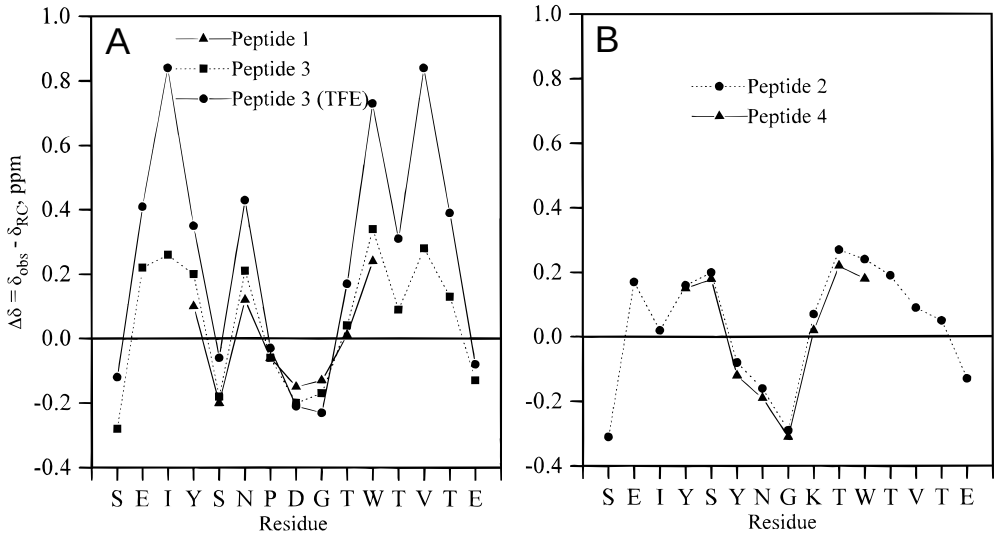

Fig. 5. Conformational shifts as a function of sequence for (**A**) peptide 1 (de Alba et al., 1996) and 3 in aqueous solution at pH 5.3 and 5 °C, and peptide 3 in 30% TFE at pH 5.5 and 10 °C, and (**B**) peptide 2 in aqueous solution at pH 4.3 and 5 °C (de Alba et al., 1997a) and peptide 4 in aqueous solution at pH 5.5 and 5 °C.

by the ring current effects; S5 faces the aromatic side chain of W11 and is consecutive to that of Y4, as in the case of the equivalent S residue in peptide 1 (de Alba et al., 1996). The profiles of CαH conformational shifts in the central region of peptide 3 and in peptide 1 are very similar (Fig. 5). This result confirms that the same β-hairpin conformation is adopted by both peptides. The CαH conformational shifts of most residues are slightly larger in peptide 3 than in peptide 1, suggesting that the population of β-hairpin is greater in the longer peptide. This is probably a consequence of the larger number of stabilizing hydrogen bonds and cross-strand side-chain interactions present in peptide 3 relative to peptide 1. $^3J_{\alpha N}$ coupling constants larger than 8 Hz were measured for residues E2, I3, Y4, T10, W11, T12, V13, and T14, which are located at the β-strands.

The populations of β-hairpin structures adopted by peptides have been reported to increase in alcohol–water mixtures (de Alba et al., 1995, 1996, 1997a, 1997b; Ramírez-Alvarado et al., 1996, 1997; Maynard & Searle, 1997; Maynard et al., 1998). TFE can also produce changes in chemical shifts useful to solve the signal overlap problem present in aqueous solution by allowing the observation of additional NOEs characteristic of the β-hairpin structure. For these reasons, the conformational behavior of peptide 3 was investigated in 30% TFE. The profile of CαH conformational shifts found in 30% TFE relative to aqueous solution is identical in shape, but it shows significantly larger absolute values for most of the residues (Fig. 5). Thus, TFE, as expected, promotes an increase in the β-hairpin population. The set of long-range backbone NOEs observed in 30% TFE includes all the characteristic NOEs expected for the 3:5 β-hairpin (Figs. 2A, 4C), except for three of them, CαH I3-CαH V13, CαH I3-NH T14, and NH Y4-CαH V13 NOEs, which could not be observed due to signal overlap. Long-range NOEs involving side-chain protons compatible with the expected 3:5 β-hairpin structure were also observed in 30% TFE. Relative to those observed in aqueous solution, they are more intense, which is also in agreement with an increase in β-hairpin population.

Although NOEs cannot be interpreted in terms of a unique structure because of the conformational averaging present in peptides, it is useful to calculate an ensemble of structures compatible with the NOE constraints so as to visualize the conformational properties of the favored family of structures. To this end we performed structure calculations on the basis of the distance constraints provided by the nonsequential NOEs observed for peptide 3. Intraresidue and sequential NOEs were excluded because their intensities are the ones most affected by the conformational averaging due to the contribution of random coil conformations to their intensities. Since the qualitative analysis of the NMR parameters indicates that peptide 3 adopts the same 3:5 β-hairpin in both solvents, nonsequential backbone NOEs observed in 30% TFE were included in the structure calculation. A listing of all NOEs used for the structure calculation is available in Supplementary material in Electronic Appendix (Table 4). For those residues with $^3J_{\text{C}\alpha\text{H-NH}} > 8.0$ Hz, ϕ angles were restricted to the range $-160°$ to $-80°$. The RMSD of the best 20 calculated structures was 0.9 ± 0.2 Å for backbone atoms and 1.7 ± 0.3 Å for all heavy atoms (Fig. 6). Most of the best 20 structures contain a NH N6-CO T10 hydrogen bond and about half of them one between the NH of G9 and the CO of N6. This agrees with the β-hairpin being of type 3:5 (Fig. 2A; Sibanda & Thornton, 1985, 1991; Sibanda et al., 1989). The ϕ,ψ angles of turn residues are also in agreement with the loop being a type I + G1 β-bulge turn, which is the one most frequently found in 3:5 β-hairpins (Sibanda & Thornton, 1985, 1991; Sibanda et al., 1989).

Peptide 4 adopts the two expected 2:2 β-hairpin conformations

Three long-range NOEs involving CαH protons were identified in ROESY spectra recorded for peptide 4 in D_2O (Fig. 7). The one between the CαH protons of S5 and T10 indicates the presence of a 2:2 hairpin with YNGK as turn residues (Fig. 2B), and the other two, CαHY6-CαHW11 and CαHY4-CαHV13 NOEs, are characteristic of a 2:2 hairpin with NGKT as turn residues (Fig. 2C). This result indicates that pentadecapeptide 4 adopts two 2:2 hairpins similar to those adopted by its shorter analogue, decapeptide 2. No more of the expected long-range NOEs for the two 2:2 β-hairpins

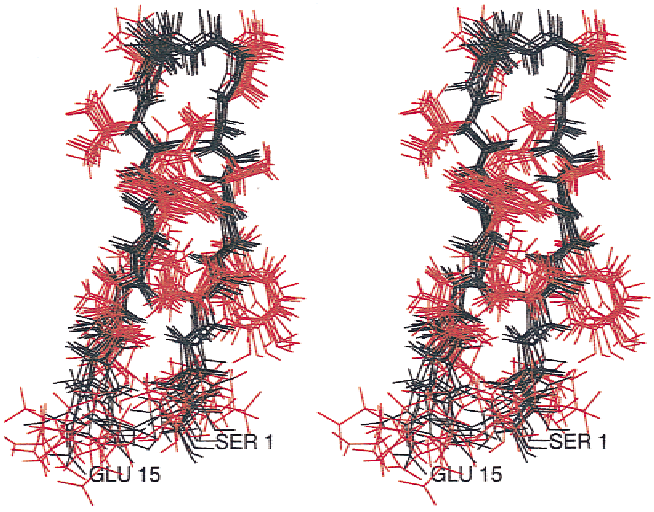

Fig. 6. Stereoscopic view of the superposition of all heavy atoms of the best 20 calculated structures for the 3:5 β-hairpin adopted by peptide 3. Backbone atoms are shown in black lines and side-chain atoms in red.

could be observed. This is probably a consequence of the poor signal to noise ratio of NOESY and ROESY spectra of peptide 4 in H_2O/D_2O 9:1 caused by the low peptide solubility. Concerning the CαH conformational shifts, those observed for peptide 4 in aqueous solution are negative for residues YNG at the turn region and positive for segments E2-S5 and K9-T14 (Fig. 5), in agreement with those expected for β-hairpins. As mentioned already, the N- and C-terminal residues are not considered due to end effects. Interestingly, the profiles of CαH conformational shifts found for peptides 3 and 4 differ significantly. However, the profiles of the common sequence of pentadecapeptide 4 relative to decapeptide 2 share the same shape (Fig. 5), as occurred with peptide 3 relative to peptide 1. In the case of peptides 4 and 2, even the absolute values of the CαH conformational shifts are almost identical. This indicates that the overall population of β-hairpin structures is approximately the same in both peptides, which is not surprising if we consider that the sum of the populations estimated for the two distinct 2:2 β-hairpins adopted by peptide 2 is close to 90% (de Alba et al., 1997a).

Peptide 5 exists as two species, an aggregated state and a monomeric one, in slow equilibrium. The monomeric state forms the expected 3:5 β-hairpin conformation

The pattern of NOEs observed for peptide 5 at pH 2.2, where only the monomer is present, includes a NH S2-NH T14 NOE as well as NOEs involving the side-chain protons of residues I3 and W11, residues facing each other in the expected β-hairpin (Fig. 2A; Table 5 in Supplementary material in Electronic Appendix). Thus, the set of long-range NOE connectivities indicates the formation of the expected 3:5 β-hairpin (Fig. 2A). The profile of CαH conformational shifts at pH 2.2 (Fig. 8) is also in agreement with the formation of a β-hairpin. The population of the β-hairpin must be low as suggested by the small absolute values of the CαH conformational shifts. Thus, the absence of some expected NOEs involving the backbone protons is probably due to the low β-hairpin population. The similarity of the $\Delta\delta_{C\alpha H}$ profile of peptide 5 with that previously reported for peptide 1 (Fig. 8; de Alba et al., 1996) indicates that both adopt the same type of β-hairpin structure.

The β-hairpin populations of some peptides containing the NPDG turn sequence decrease at low pH as a consequence of a side-chain–side-chain N-D interaction (de Alba et al., 1995, 1996). Therefore, the population of 3:5 β-hairpin adopted by peptide 5, which has the NPDG turn sequence, is expected to increase at pH values higher than 2.2. But, as already mentioned, two species coexist at pH 4.3 due to self-association. The similar δ-values of the monomer species observed at pH 2.2 and of the major species

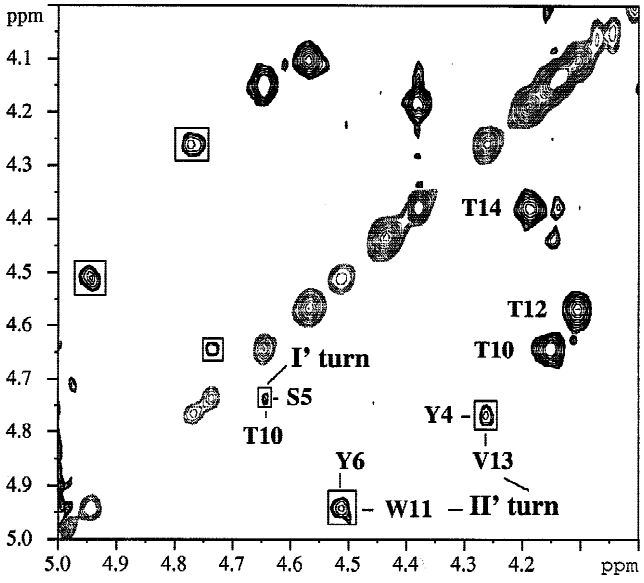

Fig. 7. ROESY spectral region of peptide 4 (1 mM, D_2O, pH 6.3, 5 °C, 200 ms mixing time). Nonsequential cross peaks are boxed. Negative contour levels are indicated by dotted lines.

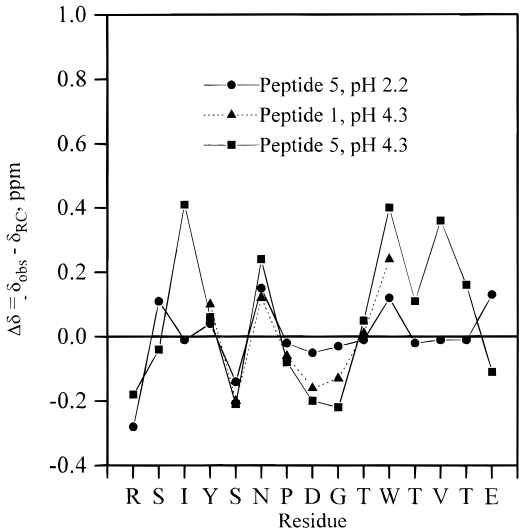

Fig. 8. Conformational shifts as a function of sequence for peptide 1 (de Alba et al., 1996) and 5 in aqueous solution at pH 4.3 and 5 °C, and for peptide 5 in aqueous solution at pH 2.2 and 5 °C.

present at pH 4.3 indicate that the latter must be also monomeric. Since assignment of this major species at pH 4.3 was feasible (see above), we analyzed its NMR data in structural terms. The profile of CαH conformational shifts corresponding to the major species of peptide 5 at pH 4.3 (Fig. 8) fits well with the formation of a β-hairpin, since it shows negative values in the turn region and positive in the strands. The negative $\Delta\delta_{C\alpha H}$ value observed for S5 has been found previously for this same residue in peptides 1 and 3 (Fig. 8; de Alba et al., 1996). The ring current effect of the aromatic side chain of its facing residue in the β-hairpin, W11, or of its neighbor residue, Y4, can account for the observed $\Delta\delta_{C\alpha H}$. The absolute values of the CαH conformational shifts of peptide 5 at pH 4.3 are larger than those observed at pH 2.2 and than those of peptide 1 (Fig. 8). This indicates that, as expected, the population of β-hairpin adopted by the monomeric species of peptide 5 increases at pH 4.3. Under the same experimental conditions, pentadecapeptide 5 adopts a higher population of 3:5 β-hairpin than decapeptide 1. This can be explained by the larger number of stabilizing hydrogen bonds and cross-strand side-chain interactions present in peptide 5, as suggested in the case of peptide 3 (see above). The long-range NOEs involving backbone NH protons, S2-T14 and Y4-T12, and side-chain protons of residues Y4-T12, Y4-T14, I3-W11, and S5-W11 that were identified at pH 4.3 (Table 5 in Supplementary material in Electronic Appendix) are compatible with the expected 3:5 β-hairpin (Fig. 2A). However, this is not conclusive evidence since it is impossible to distinguish if the long-range NOEs are intra- or intermolecular due to chemical exchange between protons in the major monomeric species and in the minor self-associated one.

Discussion

The paper presents three distinct objectives. (1) The design of pentadecapeptides able to form monomeric β-hairpins in aqueous solution. (2) The study of the effect of salt bridges on β-hairpin stability. (3) The investigation of the effect of changing the turn sequence in the β-hairpin structure. Concerning the first two objectives, two different peptides (peptides 3 and 5 in Fig. 1) were designed. A potentially stabilizing cross-strand R-E salt bridge was introduced in the sequence of peptide 5. Two species of peptide 5, a monomeric state and a self-associated one, are in slow equilibrium at the NMR time scale under most experimental conditions. The population of the associated state is pH dependent, since it vanishes at pH 2.2 and 9.3, and is maximal at about pH 5.3. Thus, the optimal conditions for self-association of peptide 5 are close to the peptide pI and coincide with the R1 guanidinium side-chain group and the N-terminus being positively charged and the E, D, and terminal carboxylate groups being negatively charged. The intrinsic pK_a values for the R guanidinium side-chain group, the N-terminal amino group, the E side-chain carboxylate, the D side-chain carboxylate, and the C-terminal carboxylate are 12, 7.7, 4.5, 4.0, and 3.6, respectively (Tanford, 1968; States & Karplus, 1987). It is known that proteins can be less soluble and even precipitate when the pH equals their pI, as a consequence of having a zero net charge. Nevertheless, peptide 5 aggregates over a very broad pH range (self-associated species are observed from pH 3.5 to 7.5), so that aggregation persists under conditions where the peptide charge is larger than 1 (positive at pH 3.5 and negative at pH 7.5). Therefore, proximity of the pH value to the peptide pI value does not seem to be the only cause for aggregation. Moreover, some other previously reported β-hairpin-forming peptides (a ubiquitin-derived 16-residue peptide, Searle et al., 1995; a designed 10-residue peptide, de Alba et al., 1996) did not aggregate under experimental conditions very close to their corresponding pI value. The formation of intermolecular salt bridges is the most likely additional driving force for self-association of peptide 5. Similar pH-dependent behaviors observed in other β-sheet forming peptides were attributed to intermolecular salt bridges (Muga et al., 1990). Hydrophobic effects may also be contributing to peptide 5 aggregation. NMR data on the monomeric state of peptide 5 indicate that the monomer adopts the expected 3:5 β-hairpin structure (see above). The available NMR data on the associated state are not sufficient to determine if the peptide aggregates in its structured form or in a random one. On the whole, although able to adopt the target structure, peptide 5 is not valid as a β-hairpin model due to its tendency to aggregate. Cross-strand charged–charged interactions (DK, DR, EK, and ER) are favored according to statistical analysis of pair frequencies in protein antiparallel β-sheets (Lifson & Sander, 1980; Wouters & Curmi, 1995; Gunasekaran et al., 1997; Hutchinson et al., 1998) and hence, they could be considered suitable for β-sheet peptide design. The pairs ER and EK in a hydrogen-bonded site of an antiparallel β-sheet were also found to be the most stabilizing pairs in an experimental investigation (Smith & Regan, 1995). Our results, however, suggest that the use of salt bridges in the design of monomeric β-sheet or β-hairpin forming peptides should be accompanied by additional design solubility criteria to avoid peptide aggregation. Since many sequences with a high propensity to form β-sheets also have a strong tendency to aggregate, design of monomeric β-sheet forming peptides must disfavor aggregation and not only include favorable interactions, as stated by Smith and Regan (1997).

In contrast to peptide 5, peptide 3 is monomeric in aqueous solution and adopts the expected 3:5 β-hairpin (Fig. 2A), as demonstrated by the NMR data. The absence of aggregation in peptide 3, for which design solubility criteria were a top priority, shows that this factor is essential in the design of monomeric β-hairpin forming peptides. Solubility criteria were indeed considered in the design of peptides reported to adopt monomeric β-hairpin structures in aqueous solution (de Alba et al., 1996; Ramírez-Alvarado et al., 1996; Smith & Regan, 1997).

Pentadecapeptide 3 is a good β-hairpin model that can be used for analysing the effect of turn residue substitutions. Out of the various substitutions previously done in the model decapeptide 1, we have performed the one producing the most drastic change in terms of peptide's conformational behavior. Pentadecapeptide 3, as decapeptide 1, contains the NPDG turn sequence, which at each position has the highest intrinsic tendencies in a type I turn (Wilmot & Thornton, 1988) and forms a 3:5 β-hairpin with a type I + G1 β-bulge. Pentadecapeptide 4 and decapeptide 2, both with the NPDG sequence substituted by YNGK, adopt two 2:2 β-hairpin conformations, one with a type I′ turn formed by residues YNGK, each residue has the highest propensity to form a type I′ turn (Hutchinson & Thornton, 1994), and the other with a type II′ turn (residues NGKT), where G and T are the residues with the highest tendencies to be at positions $i + 1$ and $i + 3$, respectively, of a type II′ turn (Hutchinson & Thornton, 1994). The conformational behavior of peptides 3 and 4 indicates that, as previously found in decapeptides (de Alba et al., 1996, 1997a, 1997b), the turn sequence is essential in defining the type of β-hairpin to be adopted. Since the three β-hairpins adopted by peptides 3 and 4 contain the same number of backbone hydrogen bonds (Fig. 2), increasing β-hairpin stability by forming a larger number of backbone hy-

drogen bonds is not driving the formation of different β-hairpins in peptides 3 and 4. The fact that strands in our peptide system are longer than the average length of strands in protein β-hairpins (Sibanda & Thornton, 1991; Ramírez-Alvarado et al., 1996) suggests that the role of turn residues in β-hairpin stability offsets that of strand residues. It could be argued that the β-turn sequence is directing β-strand alignment only because specific, favorable cross-strand side-chain–side-chain interactions are absent. To respond to this, a peptide with optimized side-chain–side-chain interactions would be very helpful. But, optimization of side-chain–side-chain interactions would probably lead to peptide insolubility or aggregation or both, given that most of the amino acids taking part in the favorable cross-strand interactions are very hydrophobic. Therefore, we have analyzed the cross-strand pairs of the three β-hairpins in terms of their reported statistical probabilities in protein antiparallel β-sheets (Hutchinson et al., 1998) and considering only residue pairs with statistically significant values. The 2:2 β-hairpin with a type I′ β-turn (Fig. 2B) contains two stabilizing cross-strand interactions (S-T in a nonhydrogen-bonded site). The 3:5 β-hairpin with a type I + G1 β-bulge turn (Fig. 2A) has one (I-V, which is favorable in β-hairpins as analyzed by Gunasekaran et al., 1997, and is favorable in a nonhydrogen-bonded site according to Wouters & Curmi, 1995, but not statistically significant in the analysis of Hutchinson et al., 1998). The 2:2 β-hairpin with a type II′ β-turn (Fig. 2C) contains no stabilizing interaction (it would have one if we consider Y-W in a nonhydrogen-bonded site that is favorable but not statistically significative according to either Hutchinson et al., 1998 or Wouters & Curmi, 1995). Thus, if favorable cross-strand interactions were directing β-hairpin formation, peptide 3 would adopt a 2:2 β-hairpin, which is not detected. The sequence at the turn, is compatible with the formation of a 2:2 β-hairpin, since the NPDG sequence would adopt a type I β-turn, and 2:2 hairpins with that type of turn are found in proteins (Sibanda & Thornton, 1985, 1991; Sibanda et al., 1989). Nevertheless, the type I β-turn lacks the right-handed twist appropriate for β-sheet structures and the formation of a type I + G1 β-bulge turn, which has the right-handed twist, drives β-hairpin formation in peptide 3 and compensates for the smaller number of favorable cross-strand interactions. Type I′ and type II′ β-turns are right-handed twisted. Peptide 4, which has a sequence that can adopt a type I′ β-turn and a one-residue-shifted II′ β-turn (Fig. 2B,C), forms the two possible 2:2 β-hairpins in spite of having less favorable cross-strand interactions in the 2:2 β-hairpin with a type II′ β-turn. Thus, our results demonstrate that the turn sequence not only affects β-hairpin stability as recently reported in other peptide models (de Alba et al., 1997a, 1997b; Haque & Gellman, 1997; Ramírez-Alvarado et al., 1997), but also, at least in our peptide systems, can define the type of β-hairpin and the strand register. Results on ubiquitin-derived peptides agree with our proposal. They showed that replacement of the native turn of the 17-residue N-terminal β-hairpin by NPDG leads to a 3:5 β-hairpin with a non-native strand register (Searle et al., 1995) whereas its substitution by VDPGO, which forms a type II′ β-turn, drives to the formation of a 2:2 β-hairpin with native strand alignment (Stanger & Gellman, 1998). Nevertheless, further experimental work in other peptide systems will be needed to prove the generality of our proposal regarding the essential role of the turn sequence in β-hairpin formation. This conclusion is also in agreement with β-hairpin formation being initiated at the β-turn, as suggested by theoretical studies (Muñoz et al., 1997, 1998). Since experimental studies on the folding of a small β-sheet protein support the idea that β-hairpins are initiation sites for β-sheet formation (Shönbrunner et al., 1997), our results on β-hairpin formation are particularly relevant for the folding of β-sheet proteins.

Conclusions

From the ^{1}H NMR analysis of the conformational behavior of three designed pentadecapeptides, we have been able to draw the following conclusions: The introduction in the design of potentially stabilizing salt bridges may provoke aggregation. The two monomeric peptides adopt the β-hairpin conformation expected for their turn sequence, which demonstrates that turn sequence is more important than side-chain interactions in determining the type of β-hairpin. Thus, at least in the investigated peptide systems, turns direct the pairing of the strands in β-hairpins, and consequently the relative orientation of the side chains of their constituent residues. This result, if generally valid, may have strong implications for the folding of proteins whose native structure contains β-hairpin motifs.

Materials and methods

Peptide synthesis and purification

Peptides 3 and 5 were chemically synthesized by the Peptide Synthesis Facility at the Department of Organic Chemistry (University of Barcelona, Spain) and peptide 4 by American Peptide Company (Sunnyvale, California). 2,2,2-Trifluoroethanol-d_3 was purchased from Cambridge Isotopes Laboratories (Cambridge, Massachusetts).

Sedimentation equilibrium

Sedimentation equilibrium experiments were performed to obtain the average molecular weight of peptide samples at the concentrations used in the NMR experiments and 150 mM NaCl to screen nonideal effects involving charged residues at high peptide concentrations. Peptide samples (30 μL) were centrifuged at 40,000 rpm at 278 and 281 K (in the case of peptide 5) in 4 mm triple-sector Epon charcoal centrepieces, using a Beckman Optima XL-A ultracentrifuge with a Ti60 rotor. Radial scans were taken at different wavelengths every 2 h until equilibrium was reached. The data were analyzed using the program XLAEQ from Beckman. The partial specific volumes of the peptides were calculated on the basis of their amino acid composition and corrected for temperature (Laue et al., 1992). They were 0.706 and 0.701 mL/g for peptide 3 and 4, respectively, at 5 °C and 0.714 mL/g for peptide 5 at 8 °C.

^{1}H-NMR spectra

Peptide samples for NMR experiments were prepared in 0.5 mL of H_2O/D_2O (9:1 ratio by volume) or in pure D_2O. Peptide concentration depended on peptide solubility. pH was measured with a glass micro electrode and was not corrected for isotope effects. The temperature of the NMR probe was calibrated using a methanol sample. Sodium [3-trimethylsilyl 2,2,3,3-^{2}H] propionate (TSP) was used as an internal reference. The ^{1}H-NMR spectra were acquired on a Bruker AMX-600 pulse spectrometer operating at a proton frequency of 600.13 MHz. 1D spectra were acquired using 32 K data points, which were zero-filled to 64 K data points before performing the Fourier transformation. Phase-sensitive 2D total

correlated spectroscopy (TOCSY) (Rance, 1987), nuclear Overhauser enhancement spectroscopy (NOESY) (Jeener et al., 1979; Kumar et al., 1980) and rotating frame nuclear Overhauser effect spectroscopy (ROESY) (Braunschweiler & Ernst, 1983; Bothner-By et al., 1984) spectra were recorded by standard techniques using presaturation of the water signal and the time-proportional phase incrementation mode (Redfield & Kuntz, 1975). A mixing time of 200 ms was used for NOESY and ROESY spectra. TOCSY spectra were recorded using 80 ms MLEV 16 with z filter spin-lock sequence (Rance, 1987). Acquisition data matrices were defined by 2,018 × 512 points in t_2 and t_1, respectively. Data were processed using the standard XWIN-NMR Bruker program on a Silicon Graphics computer. The 2D data matrix was multiplied by a square-sine-bell window function with the corresponding shift optimized for every spectrum and zero-filled to a 2 × 1 K complex matrix prior to Fourier transformation. Baseline correction was applied in both dimensions.

Structure calculation

Intensities of medium- and long-range NOEs were evaluated qualitatively and used to obtain upper limit distant constraints: strong (3 Å), intermediate between strong and medium (3.5 Å), medium (4 Å), intermediate between medium and weak (4.5 Å), weak (5 Å), and very weak (5.5 Å). Pseudo atom corrections were added where necessary. The ϕ angles were constrained to the range $-180°$ to 0° except for Asn and Gly. For those residues with $^3J_{C\alpha H\text{-}NH} >$ 8.0 Hz, ϕ angles were restricted to the range $-160°$ to $-80°$. Structures were calculated on a Silicon Graphics computer using the program DIANA (Günter et al., 1991).

Supplementary material in Electronic Appendix

Three tables listing the δ values of peptides 3–5 (Tables 1–3), three tables listing the nonsequential NOEs observed for peptides 3–5 (Tables 4–6). Two figures showing the ultracentrifugation data for peptide 5 under experimental conditions where the peptide is monomeric (pH 2.2; Fig. 1) and under conditions where the peptide aggregates (pH 4.3; Fig. 2).

Acknowledgments

We thank Mrs. C. López, Mr. A. Gómez, and Mr. L. de la Vega for their technical assistance, and Dr. G. Rivas and Mr. J.A. Evangelio for the use of the Beckman Optima XL-A ultracentrifuge. We are grateful to Dr. D.V. Laurents for his critical reading of the manuscript. This work was supported by the Spanish DGYCT project no PB93-0189 and by the EU project no CEE B104-97-2086. E.d.A. was recipient of a predoctoral fellowship (AP93-51400679) from the Spanish Ministerio de Educación y Cultura.

References

Aurora R, Rose GD. 1998. Helix capping. *Protein Sci 7*:21–38.

Baldwin RL. 1995. α-Helix formation by peptides of defined sequence. *Biophys Chem 55*:127–135.

Blanco FJ, Jiménez MA, Herranz J, Rico M, Santoro J, Nieto JL. 1993. NMR evidence of a short linear peptide that folds into a β-hairpin in aqueous solution. *J Am Chem Soc 115*:5887–5888.

Blanco FJ, Jiménez MA, Pineda A, Rico M, Santoro J, Nieto JL. 1994a. NMR solution structure of the isolated N-terminal fragment of protein-G B1 domain. Evidence of trifluorethanol induced native-like β-hairpin formation. *Biochemistry 33*:6004–6014.

Blanco FJ, Ramírez-Alvarado M, Serrano L. 1998. Formation and stability of β-hairpin structures in polypeptides. *Curr Opin Struct Biol 8*:107–111.

Blanco FJ, Rivas G, Serrano L. 1994b. A short linear peptide that folds into a native stable β-hairpin in aqueous solution. *Nature Struct Biol 1*:584–590.

Bothner-By AA, Stephens RL, Lee JM, Warren CD, Jeanloz RW. 1984. Structure determination of a tetrasaccharide: Transient nuclear Overhauser effects in the rotating frame. *J Am Chem Soc 106*:811–813.

Braunschweiler L, Ernst RR. 1983. Coherence transfer by isotropic mixing: Application to proton correlation spectroscopy. *J Magn Reson 53*:521–528.

Bundi A, Wüthrich K. 1979. ^{1}H NMR parameters of the common amino acid residues measured in aqueous solution of linear tetrapeptides H-Gly-Gly-X-Ala-OH. *Biopolymers 18*:285–297.

Case DA, Dyson HJ, Wright PE. 1994. Use of chemical shifts and coupling constants in nuclear magnetic resonance structural studies on peptides and proteins. *Methods Enzymol 239*:392–416.

Chou PY, Fasman GD. 1974. Conformational parameters for amino acids in helical, β-sheet, and random coil regions calculated from proteins. *Biochemistry 13*:211–222.

Cox JPL, Evans PA, Packman LC, Williams DH, Woolfson DN. 1993. Dissecting the structure of a partially folded protein. Circular dichroism and nuclear magnetic resonance studies of peptides from ubiquitin. *J Mol Biol 234*:483–492.

de Alba E, Blanco FJ, Jiménez MA, Rico M, Nieto JL. 1995. Interactions responsible for the pH dependence of the β-hairpin conformational population formed by a designed linear peptide. *Eur J Biochem 233*:283–292.

de Alba E, Jiménez MA, Rico M, Nieto JL. 1996. ^{1}H NMR conformational investigation of designed short linear peptides able to fold into β-hairpin structures in aqueous solution. *Folding Design 1*:133–144.

de Alba E, Jiménez MA, Rico M. 1997a. Turn residue sequence determines β-hairpin conformation in designed peptides. *J Am Chem Soc 119*:175–183.

de Alba E, Rico M, Jiménez MA. 1997b. Cross-strand side-chain interactions versus turn conformation in β-hairpins. *Protein Sci 6*:2548–2560.

Dyson HJ, Wright PE. 1991. Defining solution conformations of small linear peptides. *Annu Rev Biophys Chem 20*:519–538.

Dyson HJ, Wright PE. 1993. Peptide conformation and protein folding. *Curr Opin Struct Biol 3*:60–65.

Gellman SH. 1998. Minimal model systems for β-sheet secondary structure in proteins. *Curr Opin Struct Biol 2*:717–725.

Gunasekaran K, Ramakrishnan C, Balaram P. 1997. β-hairpins in proteins revisited: Lessons for *de novo* design. *Protein Eng 10*:1131–1141.

Günter P, Braun W, Wüthrich K. 1991. Efficient computation of three-dimensional protein structures in solution from nuclear magnetic resonance data using the program DIANA and the supporting programs CALIBA, HABAS and GLOMSA. *J Mol Biol 217*:517–530.

Haque TS, Gellman SH. 1997. Insights on β-hairpin stability in aqueous solution from peptides with enforced type I′ and type II′ β-turns. *J Am Chem Soc 119*:3301–3302.

Hutchinson EG, Thornton JM. 1994. A revised set of potentials for β-turn formation in proteins. *Protein Sci 3*:2207–2216.

Hutchinson G, Sessions RB, Thornton JM, Woolfson DN. 1998. Determinants of strand register in antiparallel β-sheets of proteins. *Protein Sci 7*:2287–2300.

Jeener J, Meier BH, Bachmann P, Ernst RA. 1979. Investigation of exchange processes by two-dimensional NMR spectroscopy. *J Chem Phys 71*:4546–4553.

Kim CA, Berg JM. 1993. Thermodynamic β-sheet propensities measured using a zinc-finger host peptide. *Nature 362*:267–270.

Kim PS, Baldwin RL. 1990. Intermediates in the folding reactions of small proteins. *Annu Rev Biochem 59*:631–660.

Kumar A, Ernst RR, Wüthrich K. 1980. A two-dimensional nuclear Overhauser enhancement (2D NOE) experiment for the elucidation of complete proton-proton cross-relaxation networks in biological macromolecules. *Biochem Biophys Res Commun 95*:1–6.

LaBrenz SR, Kelly JW. 1995. Peptidomimetic host that binds a peptide guest affording a β-sheet structure that subsequently self-assembles. A simple receptor mimic. *J Am Chem Soc 117*:1655–1656.

Laue TM, Shak BD, Ridgeway TM, Pelletier SL. 1992. Computer-aided interpretation of analytical sedimentation data for proteins. In: Harding SE, Rowe AJ, Horton JC, eds. *Analytical ultracentrifugation in biochemistry and polymer science*. Cambridge, UK: Royal Society of Chemistry. pp 90–125.

Lifson S, Sander C. 1980. Specific recognition in the tertiary structure of β-sheets in proteins. *J Mol Biol 139*:627–639.

Lyu PC, Wemmer DE, Zhou HX, Pinker RJ, Kallenbach NR. 1993. Capping interactions in isolated α-helices: Position-dependent substitution effects and structure of a serine-capped peptide helix. *Biochemistry 32*:421–425.

Marqusee S, Baldwin RL. 1987. Helix stabilization by $Glu^- \ldots Lys^+$ salt bridges in short peptides of *de novo* design. *Proc Natl Acad Sci USA 84*:8898–8902.

Maynard AJ, Searle MS. 1997. NMR structural analysis of a β-hairpin peptide designed for DNA binding. *Chem Commun XX*:1297–1298.

Maynard AJ, Sharman GJ, Searle MS. 1998. Origin of β-hairpin stability in solution: Structural and thermodynamics analysis of the folding of a model peptide supports hydrophobic stabilization in water. *J Am Chem Soc 120*: 1996–2007.

McDonnell JM, Fushman D, Cahill SM, Sutton BJ, Cowburn D. 1997. Solution structures of FcεRI α-chain mimics: A β-hairpin peptide and its retroenantiomer. *J Am Chem Soc 119*:5321–5328.

McRorie DK, Voelker PJ. 1993. Self-associating systems in the analytical ultracentrifuge. Fullerton, California: Beckman Instruments, Inc.

Merutka G, Stellwagen E. 1991. Effect of amino acid ion pairs on peptide helicity. *Biochemistry 30*:1591–1594.

Minor DL Jr, Kim PS. 1994. Measurement of the β-sheet-forming ropensities of amino acids. *Nature 367*:660–663.

Muga A, Surewicz WK, Wong PTT, Mantsch HH. 1990. Structural studies with the uveopathogenic peptide N derived from retianl S-antigen. *Biochemistry 29*:2925–2930.

Muñoz V, Henry ER, Hofrichter J, Eaton WA. 1998. A statistical model for β-hairpin kinetics. *Proc Natl Acad Sci USA 95*:5872–5879.

Muñoz V, Serrano L. 1994a. Elucidating the folding problem of helical peptides using empirical parameters. *Nature Struct Biol 1*:399–409.

Muñoz V, Serrano L. 1994b. Intrinsic secondary structure propensities of the amino acids, using statistical ϕ-ψ matrices: Comparison with experimental scales. *Proteins 20*:301–311.

Muñoz V, Thompson PA, Hofrichter J, Eaton WA. 1997. Folding dynamics and mechanism of β-hairpin formation. *Nature 390*:196–199.

Nesloney CL, Kelly JW. 1996. A 2,3′-substituted biphenyl-based amino acid facilitates the formation of a monomeric β-hairpin-like structure in aqueous solution at elevated temperature. *J Am Chem Soc 118*:5836–5845.

Ramírez-Alvarado M, Blanco FJ, Niemann H, Serrano L. 1997. Role of β-turn residues in β-hairpin formation and stability in designed peptides. *J Mol Biol 273*:898–912.

Ramírez-Alvarado M, Blanco FJ, Serrano L. 1996. *De novo* design and structural analysis of a model β-hairpin peptide system. *Nature Struct Biol 3*: 604–612.

Rance M. 1987. Improved techniques for homonuclear rotating-frame and isotropic mixing experiments. *J Magn Reson 74*:557–564.

Redfield AG, Kuntz SD. 1975. Quadrature fourier NMR detection: Simple multiplex for dual detection. *J Magn Reson 19*:250–254.

Rietman BH, Folkers PJM, Folmer RHA, Tesser GI, Hilbers CW. 1996. The solution structure of the synthetic circular peptide CGVSRQGKPYC. NMR studies of the folding of a synthetic model for the DNA-binding loop of the ssDNA-binding protein encoded by gene V of phage M13. *Eur J Biochem 238*:706–713.

Scholtz JM, Baldwin RL. 1992. The mechanism of α-helix formation by peptides. *Annu Rev Biophys Biomol Struct 21*:95–118.

Scholtz JM, Qian H, Robbins V, Baldwin RL. 1993. The energetics of ion-pair and hydrogen-bonding interactions in a helical peptide. *Biochemistry 32*: 9668–9676.

Searle MS, Williams DH, Packman LC. 1995. A short linear peptide derived from the N-terminal sequence of ubiquitin folds into a water-stable nonnative β-hairpin. *Nature Struct Biol 2*:999–1006.

Searle MS, Zerella R, Williams DH, Packman LC. 1996. Native-like β-hairpin structure in an isolated fragment from ferredoxin: NMR and CD studies of solvent effects on the N-terminal 20 residues. *Protein Eng 9*:559–565.

Shönbrunner N, Pappenberger G, Scharf M, Engels J, Kiefhaber T. 1997. Effect of preformed correct tertiary interactions on rapid two-state Tendamistat folding: Evidence for hairpins as initiation sites for β-sheet formation. *Biochemistry 36*:9057–9065.

Sibanda BL, Blundell TL, Thornton JM. 1989. Conformation of β-hairpins in protein structures. A systematic classification with applications to modelling by homology, electron density fitting and protein engineering. *J Mol Biol 206*:759–777.

Sibanda BL, Thornton JM. 1985. β-hairpin families in globular proteins. *Nature 316*:170–174.

Sibanda BL, Thornton JM. 1991. Conformation of β-hairpins in protein structures. Classification and diversity in homologous structures. *Methods Enzymol 202*:59–82.

Smith CK, Regan L. 1995. Guidelines for protein design. The energetics of β-sheet side chain interactions. *Science 270*:980–982.

Smith CK, Regan L. 1997. Construction and design of β-sheets. *Acc Chem Res 30*:153–161.

Smith CK, Withka JM, Regan L. 1994. A thermodynamic scale for the β-sheet forming tendencies of amino acids. *Biochemistry 33*:5510–5517.

Stanger HE, Gellman SH. 1998. Rules for antiparallel β-sheet design: D-Pro-Gly is superior to L-Asn-Gly for β-hairpin nucleation. *J Am Chem Soc 120*: 4236–4237.

States DJ, Karplus M. 1987. A model for electrostatics effects in proteins. *J Mol Biol 197*:122–130.

Swindells MB, MacArthur MW, Thornton JM. 1995. Intrinsic ϕ, ψ propensities of amino acids, derived from the coil regions of known structures. *Nature Struct Biol 2*:596–603.

Tanford C. 1968. Protein denaturation. *Adv Protein Chem 23*:121–283.

Wilmot CM, Thornton JM. 1988. Analysis and prediction of the different types of β-turn in proteins. *J Mol Biol 203*:221–232.

Wishart DS, Sykes BD. 1994. Chemical shifts as a tool for structure determination. *Methods Enzymol 239*:363–392.

Wouters MA, Curmi PM. 1995. An analysis of side chain interactions and pair correlations within antiparallel β-sheets: The differences between backbone hydrogen-bonded and non-hydrogen-bonded residue pairs. *Proteins 22*:119–131.

Wüthrich K. 1986. *NMR of proteins and nucleic acids.* New York: J. Wiley & Sons.

Wüthrich K, Billeter M, Braun W. 1984. Polypeptide secondary structure determination by nuclear magnetic resonance observation of short proton–proton distances. *J Mol Biol 180*:715–740.

Zhou NE, Kay CM, Sykes BD, Hodges RS. 1993. A single-stranded amphipathic alpha-helix in aqueous solution: Design, structural characterization, and its application for determining alpha-helical propensities of amino acids. *Biochemistry 32*:6190–6197.